AIAA 82-4031

Generation of Higher Harmonics in a Self-Oscillating Mixing Layer-Wedge System

Samir Ziada* and Donald Rockwell†
Lehigh University, Bethlehem, Pa.

The unsteady upstream influence associated with insertion of an impingement wedge in an unstable mixing layer is shown to enhance the coherence at the fundamental frequency of vortex formation, and to produce well-defined higher harmonics in a manner strikingly similar to artificial excitation of the corresponding nonimpinging flow. Each of the higher harmonic components grows at a rate 1.6 times that of the fundamental component, agreeing well with strong nonlinear interaction theory. Furthermore, assuming a state of quasiamplitude equilibrium at each streamwise station, the absolute value of each of the higher harmonic components was obtained from the Stuart perturbation model; the first harmonic amplitudes agree well with predicted values. At amplitude equilibrium, there is also very favorable agreement. Finally, a spectral analysis of the unsteady velocity expression of the Stuart model allowed comparison of measured and predicted velocity spectra; there is good agreement in both amplitude and shape of the spectra away from the center ($y_{0.5}$) of the shear layer.

Introduction

IT is well known that inviscid linear stability theory can describe the flow dynamics only as long as the disturbance amplitude ϵ is small compared with the base flow U. In agreement with the experimental findings of Browand[1] and Sato,[2] Schade's[3] nonlinear stability analysis has shown the linearity limit to be $\epsilon/U=4\%$. Beyond this limit, it is necessary to consider nonlinear and/or viscous terms in the governing vorticity equation; such considerations lead to the generation of higher harmonics of the fundamental mode of oscillation, as well as to distortion of the mean flow.[4] These nonlinear features have been observed for both artificially excited free shear layers[1,5,6] and self-excited impinging shear layers.[7-9] However, with the exception of Miksad's[6] investigation of certain aspects of artificially excited (*nonimpinging*) free shear layers, these nonlinear features have not been thoroughly investigated or compared with those of the existing nonlinear models. In addition, the possible similarities between artificially and self-excited shear layers, especially within the region of nonlinear activity, have not been clarified adequately.

The search for a plausible mechanism of transition to turbulence has encouraged the development of nonlinear stability theory in recent years.[3,4,10-13] There has been a tendency to concentrate on simplified cases such as neutral *two-dimensional* disturbances, implying either a state of amplitude equilibrium or a slowly growing disturbance. The inference that results obtained under such conditions are representative of those occurring for the most amplified disturbance in a laboratory shear layer awaits experimental validation. On the other hand, simulation of *three-dimensional* disturbances (e.g., Benney[14]), characterized by the existence of a secondary streamwise-vortex system, is also associated with generation of a first harmonic if, for example, the wavelength of this vortex system is half that of the primary vortices. With regard to this aspect, the aforementioned observations[1,5,6] of generation and growth of higher harmonics in the apparent absence of spanwise-periodic structure does not support the existence of three-dimensional nonlinear effects as a necessary condition for generation of higher harmonics. In this investigation, two-dimensional nonlinear stability theory will be considered and compared with the experimental data exhibiting a strong spanwise coherence. Where appropriate, these data, taken for those disturbances undergoing the greatest self-amplification, will be compared with those of Miksad involving artificial excitation in order to characterize the similarities between externally and self-excited shear layers. From a practical standpoint, the existence of nonlinear effects implies the presence of not only the fundamental component of oscillation (β), but also higher harmonic components (2β, 3β,...) as well. Consequently, the nature of the localized loading of the impingement surface and the far-field noise can be expected to be influenced by the higher harmonics. Of course, the energy at the fundamental is associated with the energy distributed among the higher harmonic components; in fact, Miksad[6] has demonstrated, for the case of an artificially excited *nonimpinging* mixing layer, that there is energy transfer between components as the flow evolves in the streamwise direction.

Experimental System

As shown in Fig. 1, the experimental arrangement consisted of a trailing edge separating high- and low-speed streams, allowing formation of well-defined vortices. These coherent vortical structures eventually impinged upon the downstream wedge, which was attached to a long plate to preclude parasitic effects associated with the wake of the wedge. At the wedge, the unsteady force was measured using a high-sensitivity strain gage system attached to the top end of the wire system illustrated in Fig. 1. Complete details of the experimental system are described by Ziada[15] wherein the upstream (approach) flow arrangement and particulars of the wedge/strain gage assembly are addressed. Here, relevant aspects of the instrumentation and data processing are given.

Extensive velocity measurements were taken by means of DISA hot-film probes (55T11 and 55R14) using a DISA 55D01 anemometer in conjunction with a DISA 55M25 linearizer. Velocity and force signals were filtered and amplified by Krohn-Hite Model 3700 bandpass filters and class A variable-gain amplifiers. The nominal filtering frequencies were 0.2 and 20 Hz for all measurements, whereas the typical frequencies of interest were in the range of 3.0-10.0 Hz. Spectral analysis of the velocity and force signals was per-

Received Feb. 24, 1981; revision received July 20, 1981.

*Graduate Student; presently Research Engineer, Vibration and Acoustics Laboratory, Gebrueder Sulzer AG, Winterthur, Switzerland.

†Professor of Mechanical Engineering and Mechanics, Department of Mechanical Engineering and Mechanics.

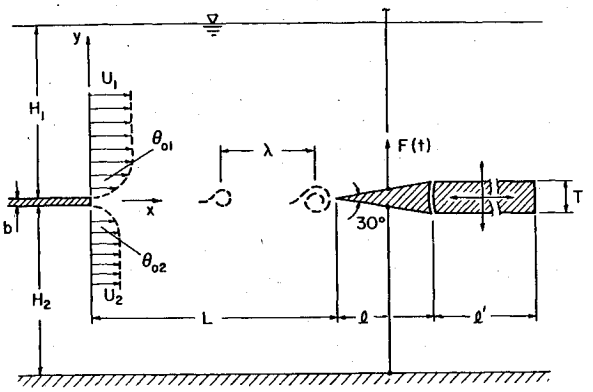

Fig. 1 Nomenclature for mixing layer-wedge system.

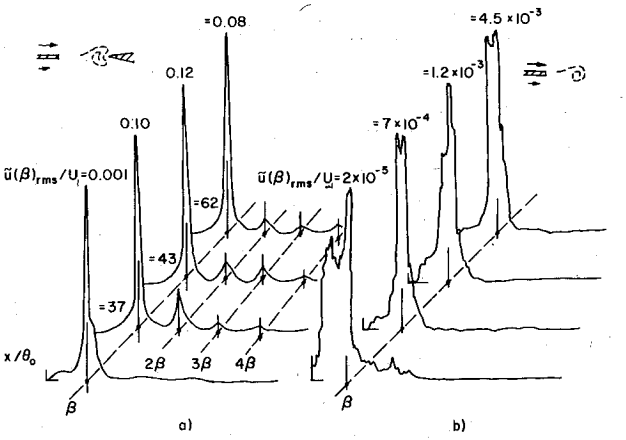

Fig. 2 Comparison of streamwise evolution of velocity spectra ($\tilde{u}_{rms}(f)/df$) at the edge of mixing layer ($\tilde{u}/U_1 = 0.9$) with and without impingement wedge: a) with impingement wedge, $L/\theta_0 = 79$; b) without impingement wedge, $L/\theta_0 = \infty$.

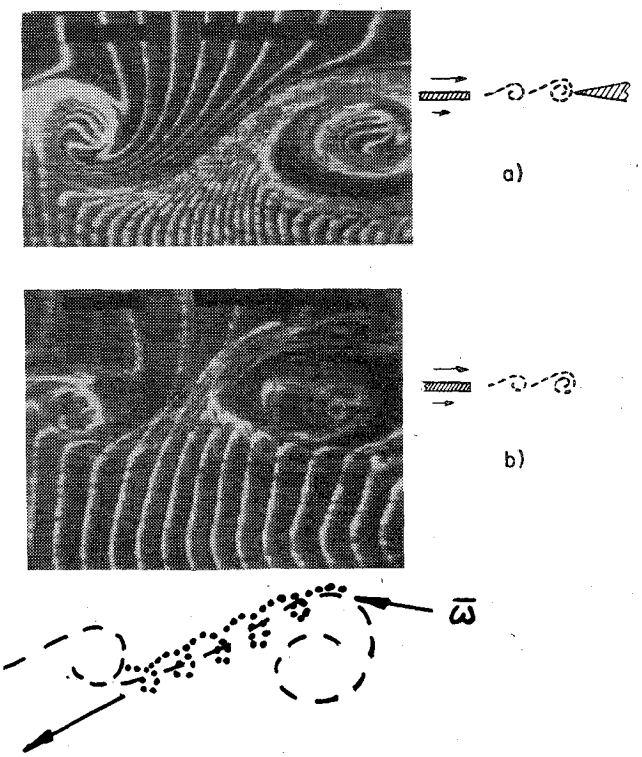

Fig. 3 Hydrogen bubble flow visualization of the mixing layer with and without impingement wedge: a) with impingement wedge, $L/\theta_0 = 79$; b) without impingement wedge, $L/\theta_0 = \infty$.

formed with the aid of a PDP-8 minicomputer. Each sample was restricted to 256 points with a sampling interval of 0.02 s. Statistical validity of the results was improved by ensemble averaging each of the 15 sample spectra. A digital oscilloscope (Nicolet 1090A) in conjunction with an *X-Y* recorder (HP7035B) were used to plot the computed spectra. All measurements were taken at a flow speed of 18.35 cm/s at the high-speed side (U_1) and velocity ratio $U_1/U_2 = 2.85 \pm 0.05$. These conditions provided extremely well-defined vortices in the downstream mixing layer with laminar boundary layers at separation having momentum thicknesses $\theta_{01} = 0.62$ mm and $\theta_{02} = 0.68$ mm, θ_0 being their sum. The corresponding Reynolds number was $Re_{(\Delta U,\theta_0)} = (U_1 - U_2)\theta_0/\nu = 157$ or $Re_{(U_1,\theta_0)} = U_1\theta_0/\nu = 239$. Other relevant parameters, defined in Fig. 1, were: $H_1/\theta_{01} = 126$, $H_2/\theta_{02} = 115$, $b/\theta_0 = 3$, $\ell'/\theta_0 = 350$, $T/\theta_0 = 15$, and $15 \le L/\theta_0 \le 150$. At this speed, the streamwise fluctuation velocity in the freestream was ~0.06%. Extensive spanwise flow visualization study showed that the flowfield was essentially two-dimensional along the entire length from separation to impingement for all impingement lengths examined.

Visualization was carried out using the hydrogen bubble method. A vertical platinum wire [0.05 mm (0.002 in.)] was used in a manner that permitted its positioning at any streamwise location. The lighting arrangement, particularly critical for effective bubble contrast, is described by Ziada.[15] The time-dependent evolution of the visualized vortex-wedge interaction and the instantaneous force fluctuation (displayed on a storage oscilloscope) were recorded simultaneously on a split-screen Instar television system having vertical and horizontal sweep frequencies of 120 and 25.2 kHz, a resolution of 250 lines, and a framing rate of 120 frames/s. Photos shown herein were obtained by taking 10.2 × 12.7 cm (4 × 5 in.) Polaroid photographs of the image on the video screen.

Experimental Observations

Before examining the nature of the higher harmonics in detail, it is appropriate to define the role of the impingement edge in altering the streamwise evolution of the unsteady shear layer. If the presence of the edge does indeed enhance the coherence of the oscillation, it can be expected to influence the strength of the higher harmonic components as well. Spectra of streamwise fluctuation velocity $\tilde{u}$ taken at the upper edge of the mixing layer ($\tilde{u}/U_1 = 0.9$, where $\bar{u}$ is the mean velocity) are shown in Fig. 2. These spectra were taken at corresponding streamwise location (x/θ_0) for the cases with and without the impingement edge. Comparison of the spectra indicates that the flowfield in the case without the edge is much less organized. This is evidenced by the spectral peaks which are wider, jagged, and of smaller amplitude. The consequence of inserting the impingement edge is to strongly enhance not only the fundamental mode β but also its higher harmonic modes as shown in Fig. 2a. Rockwell and Knisely[9] have observed a similar phenomenon for recirculating flow past a rectangular cavity with and without a downstream corner. Their results, taken together with the present observations, are evidence that the enhanced organization is not due to the tendency toward mass conservation, as occurs in the closed cavity, but rather to the intrinsic "feedback"[16] from the edge to the sensitive region of the shear layer near separation. In addition, it should be noted that similar spectra have been reported by Miksad[6] for nonimpinging mixing layers with and without sound excitation at the frequency of the fundamental mode. Thus, there is a striking similarity between the influence of impingement edge and the influence of sound excitation at a discrete frequency on enhancing the flow organization at all coexisting frequencies (β, 2β, 3β,...).

Flow visualization photos of the mixing layer with and without the impingement edge are shown in Fig. 3; for both

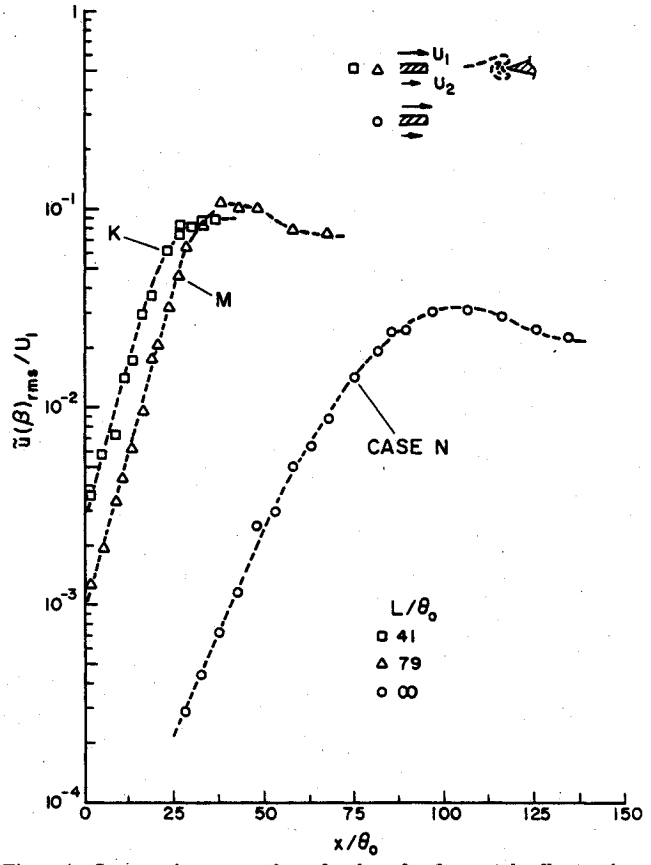

Fig. 4 Streamwise growth of the fundamental fluctuation velocity $[\tilde{u}(\beta)_{rms}/U_1]$ at edge of mixing layer ($\bar{u}/U_1 = 0.9$): case N, without wedge, $L/\theta_0 = \infty$; case K, $L/\theta_0 = 41$; case M, $L/\theta_0 = 79$.

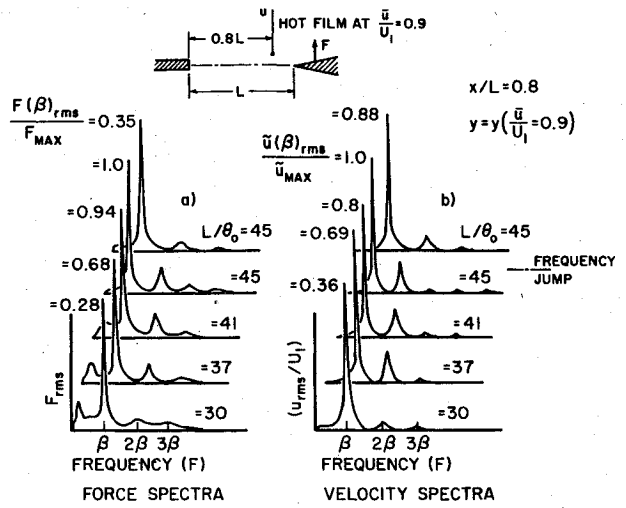

Fig. 5 Typical spectra of fluctuating force F and velocity $\tilde{u}$ for increasing impingement length L showing stage I and jump to stage II oscillation, $Re_{\theta_0} = 239$. Position of hot-film probe was adjusted to keep $x/L = 0.8$ and $\bar{u}/U_1 = 0.9$.

cases, the mean flow conditions were identical, although different hydrogen bubble pulsation rates were used. Corresponding velocity spectra for cases with and without the impingement wedge are those already shown in Fig. 2. Comparison of these two photos clearly indicates the less coherent structure, and the presence of three-dimensionality in the form of streamwise vorticity for the case without the edge. The symbol $\tilde{\omega}$ indicates the vorticity vector that has a streamwise component; the fluid possessing the vorticity $\tilde{\omega}$ is referred to as a "braid." From the corresponding video film, it is evident that as the primary (major) vortices continue to roll up, there is an increase in angular velocity of the "braid" between the primary vortices. In essence, the presence of the wedge appears to preclude or delay the onset of three-dimensionality, resulting in more coherent vortex development.

The two cases described in Fig. 2 are further contrasted in Fig. 4, which depicts the streamwise growth of $\tilde{u}(\beta)_{rms}$ measured at the edge of the shear layer ($\bar{u}/U_1 = 0.9$). Three cases are presented: the no-edge case which is designated as case N; case K corresponding to oscillations at $L/\theta_0 = 41$; and case M corresponding to oscillations at $L/\theta_0 = 79$. Comparison of cases N and M indicates that at separation and along the linear growth region the rms amplitude of fluctuation velocity for the case M exceeds that for case N by about two orders of magnitude. This can be attributed only to the substantial increase in the upstream influence and hence the enhanced flow organization consequent upon the introduction of the wedge. If the upstream influence is strongly dependent upon the vortex-edge interaction, i.e., upon the flow dynamics in the downstream region, then the vortex-edge interaction for case K should result in a larger amplitude of fluctuation velocity than that for case M, owing to the fact that in case K the induced force on the edge is larger [15] and the impingement length is shorter than those in case M. Figure 4 shows that is indeed the case. Moreover, it illustrates that the unsteady velocity field for a given impingement length can be determined neither from information at another value L nor from the case of no edge.

Now that the existence and evolution of the higher harmonic components have been characterized as a function of streamwise distance for cases with and without the impingement wedge, it is appropriate to examine the effect of impingement length scale (L/θ_0) on the nature of the higher harmonics. In addition, it is relevant to study the extent to which the force fluctuations at the impingement wedge are influenced by the higher harmonics in the incident unsteady flow.

Spectra of both the induced force F and the streamwise fluctuation velocity $\tilde{u}$ are depicted for several values of impingement length in Fig. 5. The velocity fluctuation was measured at the streamwise location $x/L = 0.8$ and at the edge of shear layer $\bar{u}/U_1 = 0.9$. As evident from Fig. 5, the general features of the force spectra are similar to those of the incident velocity fluctuation spectra: the amplitude of the spectral peak at the frequency β increases as the impingement length increases; the frequency jump is associated with a drop in amplitude of the spectral peaks; and distinct peaks exist at the frequencies of the higher harmonics. However, the quantitative relationship between force and velocity spectral peak amplitudes is not obvious. That is, as the impingement length increases, the ratio $F(\beta)_{rms}/F(2\beta)_{rms}$ increases continuously, whereas the ratio $\tilde{u}(\beta)_{rms}/\tilde{u}(2\beta)_{rms}$ appears to remain constant (~ 5.0) after an initial increase. These dissimilarities can be readily explained on the basis of the varying vortex-wedge interaction patterns as the impingement length is changed. [15] In essence, the amplitude of the induced force is a strong function of the vortex-wedge interaction pattern, whereas the maximum amplitude of the velocity fluctuations measured immediately upstream of the wedge are weakly related to the interaction pattern. Consequently, no direct quantitative relation between $\tilde{u}(\beta)_{rms}$ and $F(\beta)_{rms}$ is expected. Concerning the ratio $\tilde{u}(\beta)_{rms}/\tilde{u}(2\beta)_{rms}$, which remains constant at a value of 5.0 in Fig. 5, it is in excellent agreement with Stuart's perturbation theory which, along with other similar trends of $\tilde{u}$, will be discussed subsequently.

The dimensionless frequency components of the force induced at the wedge are plotted against the impingement length in Fig. 6. In this figure, the data points at each value of impingement length represent the frequencies at which clearly distinguishable peaks were observed in the corresponding force spectrum. Solid data points symbolize the dominant

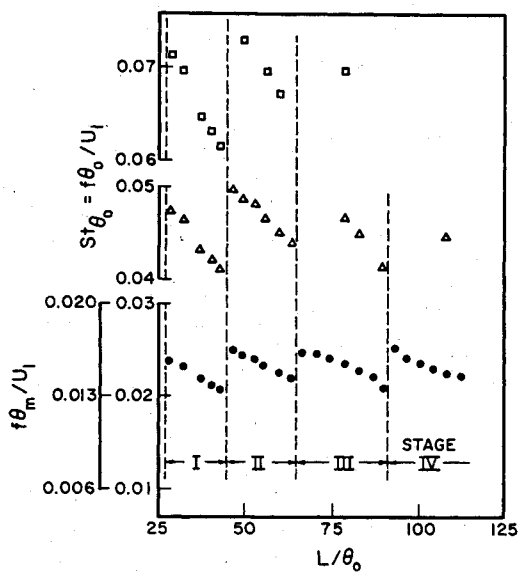

Fig. 6 Dimensionless frequencies (St_{θ_0}) of spectral peaks of fluctuating force as a function of impingement length, $Re_{\theta_0} = 239$. Solid symbols indicate dominant (fundamental) frequency β component; △, 2β component; □, 3β component.

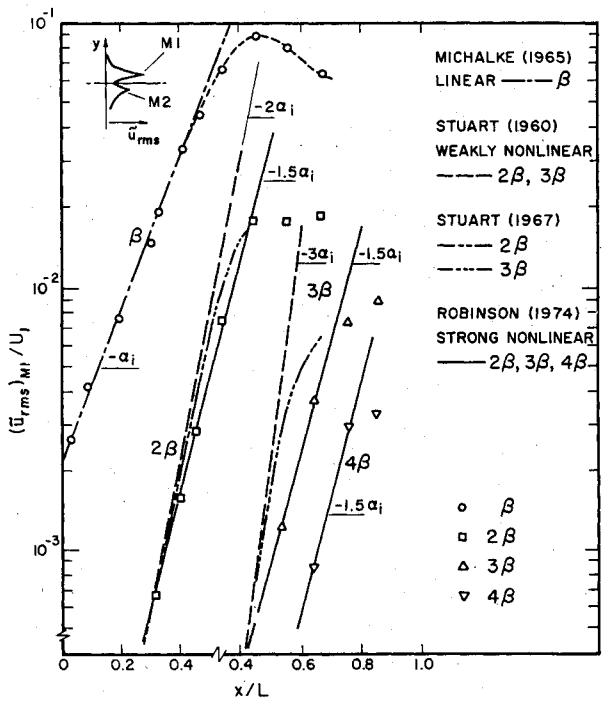

Fig. 7 Comparison of experimental and theoretical streamwise evolution of maximum fluctuation velocity components $\tilde{u}(\beta)_{M1}$, $\tilde{u}(2\beta)_{M1}$, $\tilde{u}(3\beta)_{M1}$, and $\tilde{u}(4\beta)_{M1}$ ($L/\theta_0 = 37$, $Re_{\theta_0} = 239$).

frequency components, i.e., the fundamental frequency of oscillation. The variation of Strouhal numbers, based on the momentum thickness θ_0 at separation as well as thickness θ_m (at middle of linear growth region), with the normalized impingement length are depicted. It can be seen that oscillations at the harmonic frequencies were consistently generated over most of the examined range of impingement length. This feature is similar to that of artificially excited (nonimpinging) free shear layers,[6] in that higher harmonic components were found to persist for a substantial distance downstream.

In order to investigate the streamwise evolution of the higher harmonic components relative to the fundamental,

Table 1 Criteria for onset of nonlinearity

	Investigation	Linearity limit, $\tilde{u}(\beta)_{rms}/U_1$, %
Theory	Schade[3]	4
Two-dimensional jets	Sato[2]	4
Shear layers	Browand[1]	5
Mixing layers	Miksad[6]	2
Mixing layers	Present work	2

detailed velocity spectra were taken at an impingement length $L/\theta_0 = 37$ across the shear layer at several streamwise stations. Consequently, it was possible to determine the peak amplitude of each harmonic component at a given streamwise station, designated as $\tilde{u}(\beta)_{M1}, \tilde{u}(2\beta)_{M2}, \ldots$. Figure 7 depicts the streamwise growth of the dimensionless spectral components $\tilde{u}(\beta)_{M1}, \ldots$, and $\tilde{u}(4\beta)_{M1}$; the long-short dashed line represents the prediction of $\tilde{u}(\beta)_{M1}$ based on the linear theory of Michalke[17] whereas the other lines represent various theories for predicting evolution of the higher harmonics, to be discussed shortly. The data indicate that *all the harmonic modes grow at the same growth rate,* which is 1.6 times the growth rate of their fundamental, i.e., $\alpha_i(2\beta) = \alpha_i(3\beta) = \alpha_i(4\beta) = 1.6\alpha_i(\beta)$. This result is strikingly similar to that reported for externally excited (*nonimpinging*) shear layers. Miksad[6] found that all harmonics grow nearly 1.5 times as fast as their fundamental only if the frequency of the *artificial* excitation ($\beta = 0.0177$) approximates that frequency at which the shear layer is most unstable ($\beta_{max} = 0.0167$). In the present experiment, the frequency $\beta = 0.0155$ also approximates β_{max}. For other excitation frequencies, Miksad found the growth rates of the harmonics to be in the range of 1.15-1.73 times that of their fundamental.

Concerning the linearity limit, Fig. 7 shows that the first harmonic (2β) is first detected when $\tilde{u}(\beta)_{rms}/U_1$ is 2%. Table 1 compares this result with those of other investigations of artificially excited mixing layers and jets.

In the following, nonlinear stability theories are considered and contrasted with the experimental data reported herein. For purposes of discussion, the analyses are grouped into two categories: the term relative growth rate is applied to those that provide the growth rates of the higher harmonic components, but not their absolute values; by absolute growth rate is meant those that give absolute values of the higher harmonics.

Relative Growth Rates of Higher Harmonics

Consider the case of a two-dimensional neutral disturbance with a phase speed c. In a frame of reference also moving with speed c, a solution of the following form is sought

$$\psi_t = \int^y (\tilde{u}(y) - c)\,dy - \epsilon\psi(x,y) \tag{1}$$

where ψ_t and ψ are the total and disturbance stream functions, respectively; $\tilde{u}(y)$ represents the mean flow; and ϵ is a small parameter proportional to the dimensionless disturbance amplitude. Substituting in the vorticity equation yields the following disturbance equation

$$(\tilde{u}-c)\nabla^2\psi_x - \tilde{u}_{yy}\psi_x + \epsilon(\psi_y\nabla^2\psi_x - \psi_x\nabla^2\psi_y) = \nu\nabla^4\psi \tag{2}$$

When the parameters ϵ and ν are small, as in the case of inviscid linear stability theory, Eq. (2) becomes

$$(\tilde{u}-c)\nabla^2\psi_x - \tilde{u}_{yy}\psi_x = 0 \tag{3}$$

which is Rayleigh's equation and is valid everywhere except at the critical layer $y = y_c$ where $\tilde{u} = c$. This singularity of the

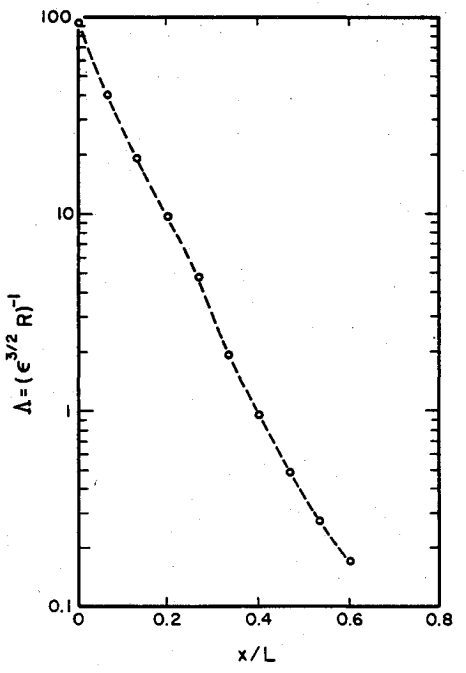

Fig. 8 Variation of the parameter Λ with streamwise distance x/L ($L/\theta_0=37$, $Re_{\theta_0}=239$).

linearized equation can be removed by using either a small linear operator of higher order which leads to the viscous theory or a small nonlinear operator which leads to the nonlinear theory.

Benney and Bergeron[12] have elaborated on this aspect; they argued that the appropriateness of each approach depends on the value of the parameter $\Lambda=1/(R_\epsilon)^{3/2}$ which is proportional to the inverse of the characteristic Reynolds number R_ϵ for the flow in the neighborhood of the critical layer.[11] If the characteristic speed of the mean flow is U, then the fluctuating velocity is ϵU. A characteristic length near the critical layer is known to be $\theta R^{-1/3}$, where θ is the local momentum thickness and $R=U\theta/\nu$. The characteristic Reynolds number R_ϵ is then $\epsilon U\theta R^{-1/3}/\nu$ and

$$\Lambda=1/(\epsilon R^{1/3})^{3/2}=(\epsilon^{3/2}R)^{-1} \tag{4}$$

For small values of R_ϵ (i.e., $\Lambda\gg 1$) viscous effects become more important than nonlinear effects in the neighborhood of the critical layer and hence the viscous theory, referred to hereafter as weak nonlinear theory, is applicable.[4] On the other hand, if R_ϵ is large (i.e., $\Lambda\ll 1$) then the nonlinear terms dominate and this requires a different approach to the problem, such as strong nonlinear interaction theory.[12,13]

At each streamwise station corresponding to the data of Fig. 7, the value of the parameter Λ was calculated from the measured streamwise fluctuation velocity $\tilde{u}(\beta)$ and local Reynolds number $R=U_1\theta_1/\nu$. The streamwise development of Λ is depicted in Fig. 8. For small x/L the value of Λ is large and weak nonlinear theory is appropriate; whereas for large x/L the value Λ is small, indicating that nonlinear effects are important. Examination of Figs. 7 and 8 illustrates that higher harmonics were observed only after the value of Λ fell below 2.0. Recalling that $\Lambda=0(1)$ acts as the boundary dividing the applicability of weak from strong nonlinear theory, then it becomes apparent that strong nonlinear theory has to be invoked to predict the streamwise growth of the higher harmonics. In fact, as will be illustrated, the observed growth rates were found to be in excellent agreement with those predicted by strong nonlinear theory.

According to *weak* nonlinear theory (e.g., Stuart[4]), *the nth harmonic mode grows at a rate n+1 times its fundamental,* i.e., $\alpha_i(2\beta)=2\alpha_i(\beta)$, $\alpha_i(3\beta)=3\alpha_i(\beta)$,..., where α_i is the growth rate. However, for a simple mixing layer, *strong* nonlinear interaction theory *predicts growth rates of 1.5 times the fundamental for all higher harmonic modes* (see Robinson).[13] The experimental observations corresponded closely with the predictions of this *strong* nonlinear theory (see Fig. 7); that is, *all* of the higher harmonics in the experiment were found to grow at the *same rate* of 1.6 times the growth rate of their fundamental. The suggestion that Λ values be used as a criterion for the choice between weak and strong nonlinear interaction theories is also supported by these empirical findings.

It should be noted that Fig. 8 is strikingly similar to Fig. 18 of Miksad's article[6] on artificially excited (nonimpinging) shear layers, again suggesting the similarity between the features of artificially and self-excited shear layers.

The above comparison is qualitative and can provide only the growth *rates* of the harmonic modes. For quantitative comparison one needs either a closed-form solution of the nonlinear vorticity equation or the value of the higher-order terms of the expanded solution. In the following, quantitative comparison is given between the experimental data and Stuart's[10] solutions of the nonlinear inviscid vorticity equation. Stuart's perturbation theory, as well as his exact solution, are considered.

Absolute Growth Rate of Higher Harmonics

Stuart[10] used the perturbation technique to find a solution for the case of neutral disturbance in mixing layers. The stream function ψ of this solution has the form

$$\begin{aligned}\psi=&\ell n\cosh y+\epsilon\,\mathrm{sech}y\cos\xi-\tfrac{1}{4}\epsilon^2\mathrm{sech}^2y\cos 2\xi\\&+\epsilon^3\{(\tfrac{2}{3}\mathrm{sech}y\ell n\cosh y-\tfrac{1}{4}\mathrm{sech}^3y)\cos\xi\\&+1/12\mathrm{sech}^3y\cos 3\xi\}+\epsilon^4\{(-\tfrac{1}{3}\mathrm{sech}^2y\ell n\cosh y\\&+\tfrac{1}{3}\mathrm{sech}^2y+\tfrac{1}{4}\mathrm{sech}^4y)\cos 2\xi-1/32\mathrm{sech}^4y\cos 4\xi\}+\ldots\end{aligned} \tag{5}$$

where ϵ is the perturbation parameter $\xi=\alpha x$, and α the wave number. Differentiating with respect to y and collecting the terms of similar wave number, one can obtain the rms amplitude distributions of the streamwise fluctuating velocity components of wave numbers α, 2α, 3α,.... These distributions are functions of ϵ, the perturbation parameter, and have the form

$$\tilde{u}(\alpha)_{\mathrm{rms}}=\frac{1}{\sqrt{2}}\frac{\partial}{\partial y}[\epsilon\,\mathrm{sech}y+\epsilon^3\tfrac{2}{3}\mathrm{sech}y\ell n\cosh y-\tfrac{1}{4}\mathrm{sech}^3y+\epsilon^5\ldots] \tag{6a}$$

$$\tilde{u}(2\alpha)_{\mathrm{rms}}=\frac{1}{\sqrt{2}}\frac{\partial}{\partial y}[\tfrac{1}{4}\epsilon^2\mathrm{sech}y+\epsilon^4(\tfrac{1}{3}\mathrm{sech}^2y\ell n\cosh y-\tfrac{1}{3}\mathrm{sech}^2y-\tfrac{1}{4}\mathrm{sech}^4y)+\epsilon^6\ldots] \tag{6b}$$

$$\tilde{u}(3\alpha)_{\mathrm{rms}}=\frac{1}{\sqrt{2}}\frac{\partial}{\partial y}\left[\frac{1}{12}\epsilon^3\mathrm{sech}^3y+\epsilon^5\ldots\right] \tag{6c}$$

$$\tilde{u}(4\alpha)_{\mathrm{rms}}=\frac{1}{\sqrt{2}}\frac{\partial}{\partial y}\left[\frac{1}{32}\epsilon^4\mathrm{sech}^4y+\epsilon^6\ldots\right] \tag{6d}$$

Obviously, this solution is valid only for a neutral disturbance which is in a state of amplitude equilibrium. However, an approach which deserves consideration is to treat each streamwise station as if it were in a state of quasiamplitude equilibrium. The significance of considering such an approach is that it may provide an absolute (quantitative) estimate for the streamwise evolution of the higher harmonic modes. The procedure adopted was as follows: at each streamwise station x/L the value of $\tilde{u}(\beta)_{\mathrm{M1}}$ was obtained

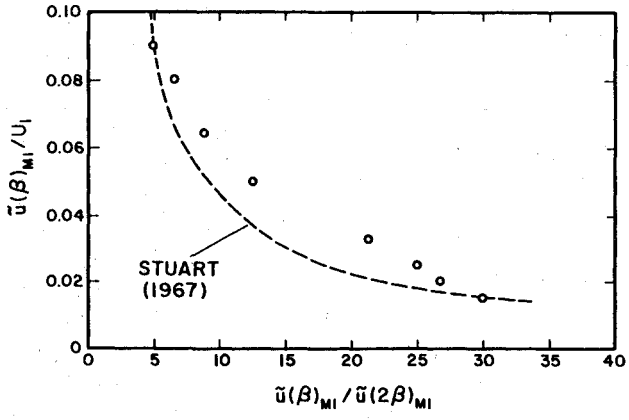

Fig. 9 Comparison of experimental and theoretical (Ref. 10) values of the ratio $\tilde{u}(\beta)_{M1}/\tilde{u}(2\beta)_{M2}$ as a function of $\tilde{u}(\beta)_{M1}(L/\theta_0=37, Re_{\theta_0}=239)$.

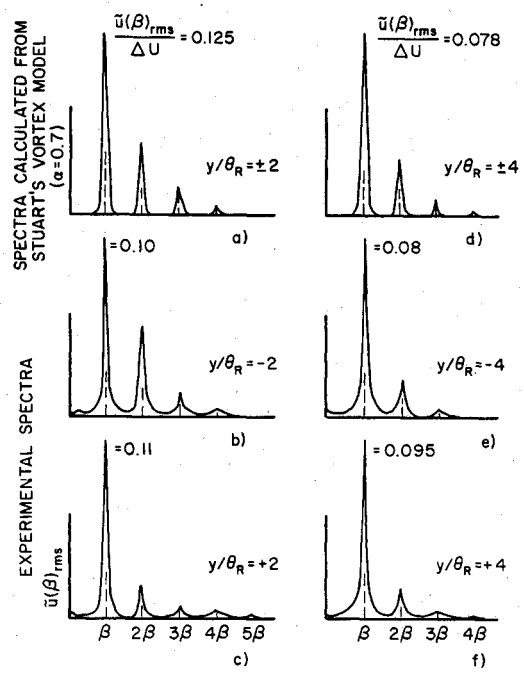

Fig. 10 Comparison of experimental and calculated spectra of fluctuation velocity $\tilde{u}$ at several transverse locations in the mixing layer ($L/\theta_0=58, x/\theta_0=46, \theta_R/\theta_0=1.46, Re_{\theta_0}=239$).

from Fig. 7; substituting $\tilde{u}(\alpha)_{\text{rms Imax}}=\tilde{u}(\beta)_{M1}$ in Eq. (6a) yielded the value of ϵ, then $\tilde{u}(2\beta)_{M1}=\tilde{u}(2\alpha)_{\text{rms Imax}}$ was obtained from Eq. (6b); likewise $\tilde{u}(3\beta)_{MI}$ was also obtained from Eq. (6c). The resultant streamwise evolutions are compared with the experimental data in Fig. 7, whereas Fig. 9 compares the measured and calculated ratio of $\tilde{u}(\beta)_{M1}/\tilde{u}(2\beta)_{M1}$. As can be seen, the calculated results well approximate the experimental data of $\tilde{u}(2\beta)_{M1}$ but not those of $\tilde{u}(3\beta)_{M1}$. It should be added that only one term in Eqs. (6) was considered in the calculation procedure. Therefore, one would expect the theory to deviate from the experimental data as $\tilde{u}(\beta)_{M1}$ (and consequently ϵ) increases due to the increased influence of the neglected higher-order terms. In fact, the agreement seems to be best when: 1) $\tilde{u}(\beta)_{M1}$ is at a maximum (i.e., saturated) and hence the assumed state of amplitude equilibrium is valid; or 2) $\tilde{u}(\beta)_{M1}$ is small and consequently the contribution of the higher-order terms is minimal.

When the value of $\tilde{u}(\beta)_{M1}$ reaches its saturation amplitude, the state of amplitude equilibrium is satisfied. Under this condition, Table 2 compares Stuart's prediction of the ratio $\tilde{u}(\beta)_{M1}/\tilde{u}(2\beta)_{M1}$ with the present and other experimental data.

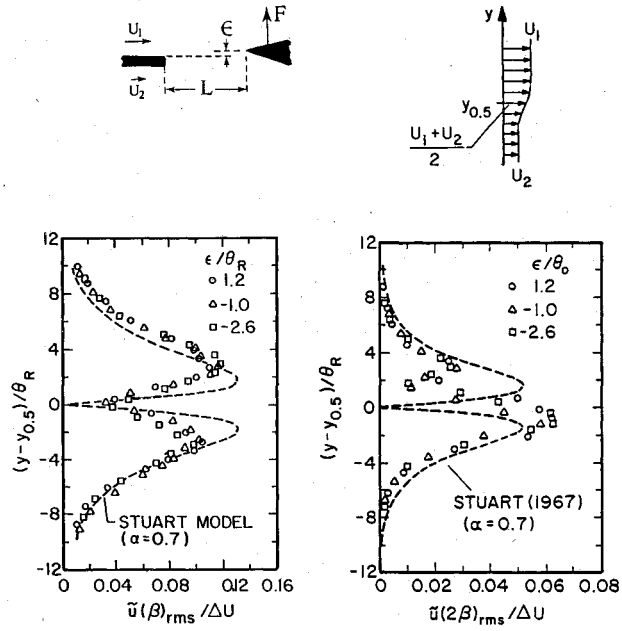

Fig. 11 Transverse distribution of fluctuation velocity components $\tilde{u}(\beta)_{rms}$ and $\tilde{u}(2\beta)_{rms}$ for different values of wedge offset ϵ in mixing layer: ---Stuart's vortex model[10] ($L/\theta_0=58, x/\theta_0=46, \theta_R/\theta_0=1.46, Re_{\theta_0}=239$).

Table 2 Amplitude ratio $[\tilde{u}(\beta)/\tilde{u}(2\beta)]$ at saturation

Investigation	Artificially excited mixing layers: Browand[1]	Artificially excited mixing layers: Miksad[6]	Self-excited mixing layers (present experiment)
Stuart's theory[10]	6	4	5.17
Experiment	5.85	5.75	5

Stuart's Exact Solution

In this section, comparison with Stuart's[10] exact solution is given, focussing on the frequency spectra of the streamwise velocity component $\tilde{u}$, as well as the characteristics of the transverse distribution of the first harmonic mode. For several values of y/θ_R ‡ streamwise velocity spectra were obtained from performing a fast Fourier transform (FFT) on a digitized form of Stuart's solution for the streamwise velocity fluctuation;[15] these spectra are contrasted with corresponding experimental spectra in Fig. 10. Since Stuart's vortex model is symmetric with respect to $y_{0.5}$, spectra of $\tilde{u}(\beta)$ are identical for $\pm y/\theta_R$. Therefore, only two spectra, *a* and *d*, for $y/\theta_R=\pm 2$ and ± 4 together with their corresponding experimental spectra are presented in Fig. 10.

Comparison of these spectra clearly indicates that the quantitative features of the vortices generated in the laboratory shear layer can be well described by the use of Stuart's vortex model. The concentration of the fluctuating energy at the frequency of the fundamental (β) and its harmonics (2β, 3β,...) is evident in both the experimental and the vortex model spectra. Moreover, the experimental values of the spectral peaks are closely predicted by the vortex model and the experimental spectra, especially the peaks at the frequency β, display symmetrical features, a trend in agreement with the vortex model.

‡θ_R is the local momentum thickness at $x/L=0.8$, where $L/\theta_0=58$; and $y_{0.5}$ is the transverse location corresponding to $\bar{u}=U_a$, where $U_a=(U_1+U_2)/2$.

The spectral peaks at the frequencies β and 2β are plotted against the transverse coordinate $(y-y_{0.5})/\theta_R$ in Fig. 11. Stuart's solution is seen to well approximate both $\tilde{u}(\beta)$ and $\tilde{u}(2\beta)$ distributions, especially in the outer range of y, i.e., for $|(y-y_{0.5})/\theta_R|>3$. Moreover, the experimental $\tilde{u}(\beta)$ distribution shows symmetric features with respect to the y coordinate, which is in agreement with not only Stuart's exact solution but also his solution obtained by employing perturbation theory. However, due to the effects associated with the upstream history of the velocity field,[15] the $\tilde{u}(\beta)$ distribution peak at negative y is somewhat smaller than that at positive y; simultaneously the $\tilde{u}(2\beta)$ distribution peak at negative y is larger than that at positive y.

Conclusion

The impingement of mixing layers on solid boundaries enhances the organization of not only the fundamental mode, but also its harmonics in a way which is very similar to that of externally excited free shear layers. All harmonic modes grow at the same rate, which is 1.6 times the growth rate of their fundamental. The first harmonic mode starts to appear when the amplitude of the fundamental disturbance is 2% of freestream velocity (this amplitude is considered to be the limit of applicability of the linear theory). For disturbance amplitudes beyond this limit, viscous and nonlinear effects become substantial and should be taken into consideration.

When the higher harmonic modes are generated, the parameter Λ, which is inversely proportional to the characteristic Reynolds number for the flow in the neighborhood of the critical layer, has an order of magnitude of unity; this suggests that nonlinear effects are more important than viscous effects and therefore strong nonlinear interaction theory is appropriate. According to this theory, all harmonics grow 1.5 times as fast as their fundamental. The excellent agreement with the experimental data supports the suggestion of Benney and Bergeron[12] that the order of magnitude of the parameter Λ be used to determine which theory should be applied.

Concerning the streamwise evolution of the amplitudes of the harmonic modes, by assuming quasi-amplitude equilibrium at each streamwise station, the results of Stuart's[10] perturbation solution provides values of the ratio $\tilde{u}(\beta)_{M1}/\tilde{u}(\beta)_{M2}$ in good agreement with experiment. Moreover, the value of this ratio at amplitude equilibrium is also well predicted. In addition, by performing spectral analysis on Stuart's expression for the unsteady velocity fluctuation, it is shown that the form and amplitude of the resultant velocity spectra are in good agreement with experimental spectra for the outer region of the shear layer.

Acknowledgments

The authors wish to express their appreciation to the National Science Foundation of Washington, D.C., and the Volkswagen Foundation of Hannover, West Germany, for financial support of this investigation. Dr. Charles Knisely and Y. P. Tang provided the computer program used in the spectral analysis, along with advice on this aspect.

References

[1] Browand, F. K., "An Experimental Investigation of the Instability of an Incompressible, Separated Shear Layer," *Journal of Fluid Mechanics,* Vol. 26, 1966, pp. 281-307.

[2] Sato, H., "The Stability and Transition of a Two-Dimensional Jet," *Journal of Fluid Mechanics,* Vol. 7, 1960, pp. 53-80.

[3] Schade, H., "Contribution to the Nonlinear Stability Theory of Inviscid Shear Layers," *Physics of Fluids,* Vol. 7, No. 5, 1964, pp. 623-628.

[4] Stuart, J. T., "On the Nonlinear Mechanics of Wave Disturbances in Stable and Unstable Parallel Flows," *Journal of Fluid Mechanics,* Vol. 9, 1960, pp. 353-370.

[5] Sato, H. and Kuriki, K., "The Mechanism of Transition in the Wake of a Thin Flat Plate Placed Parallel to a Uniform Flow," *Journal of Fluid Mechanics,* Vol. 11, 1961, pp. 321-352.

[6] Miksad, R. W., "Experiments on the Nonlinear Stages of Free Shear Layer Transition," *Journal of Fluid Mechanics,* Vol. 56, 1972, pp. 695-719.

[7] Sarohia, V., "Experimental and Analytical Investigation of Oscillations in Flows Over Cavities," Ph.D. Dissertation, California Institute of Technology, Pasadena, 1975.

[8] Hussain, A. K. M. F. and Zaman, K. B. M. Q., "The Free Shear Layer Tone Phenomenon and Probe Interference," *Journal of Fluid Mechanics,* Vol. 87, 1978, pp. 349-383.

[9] Rockwell, D. and Knisely, C., "The Organized Nature of Flow Impingement Upon a Corner," *Journal of Fluid Mechanics,* Vol. 93, 1979, pp. 413-432.

[10] Stuart, J. T., "On Finite Amplitude Oscillations in Laminar Mixing Layers," *Journal of Fluid Mechanics*, Vol. 29, 1967, pp. 417-440.

[11] Stuart, J. T., "Nonlinear Stability Theory," *Annual Review of Fluid Mechanics,* Vol. 3, 1971, pp. 347-370.

[12] Benney, D. J. and Bergeron, R. F., "A New Class of Nonlinear Waves in Parallel Flows," *Studies in Applied Mathematics,* Vol. 48, 1969, pp. 181-204.

[13] Robinson, J. L., "The Inviscid Nonlinear Instability of Parallel Shear Flows," *Journal of Fluid Mechanics,* Vol. 63, 1974, pp. 723-752.

[14] Benney, D. J., "A Nonlinear Theory for Oscillations in a Parallel Flow," *Journal of Fluid Mechanics,* Vol. 10, 1961, pp. 209-236.

[15] Ziada, S., "Self-Sustained Oscillations of a Mixing Layer-Edge System," Ph.D. Dissertation, Mechanical Engineering Department, Lehigh University, Bethlehem, Pa., 1981.

[16] Ffowcs-Williams, J. E., "Hydrodynamic Noise," *Annual Review of Fluid Mechanics,* Vol. 1, 1969, p. 197-222.

[17] Michalke, A., "On Spatially Growing Disturbances in an Inviscid Shear Layer," *Journal of Fluid Mechanics,* Vol. 22, 1965, pp. 371-383.